

Upstream influence of midlatitude jet stream biases in boreal summer

Lina Boljka^{1,2}  | Ingo Bethke^{1,2} | Dandan Tao^{1,2} | Camille Li^{1,2}

¹Geophysical Institute, University of Bergen, Bergen, Norway

²Bjerknes Centre for Climate Research, Bergen, Norway

Correspondence

Ingo Bethke, Geophysical Institute, University of Bergen, Bergen, 5020, Norway.

Email: ingo.bethke@uib.no

Funding information

Bjerknessenteret for klimaforskning, Universitetet i Bergen; Norges Forskningsråd, Grant/Award Number: 309562; Trond Mohn stiftelse, Grant/Award Number: BFS2018TMT01

Abstract

Climate models exhibit biases in the mean state and in variability across different regions of the Earth. For example, atmosphere-only models have a poleward bias in summertime jet streams across the Northern Hemisphere (NH). This can result from many processes, including misrepresentation of Rossby waves that can propagate in different directions and thereby interact with jet streams. However, Rossby-wave biases can result from biased background state of the climate system as well. The propagation speed of Rossby waves depends on jet stream strength, thus a poleward displacement of the jet stream can hinder westward propagation of Rossby waves at higher latitudes and displace eastward propagating Rossby waves (downstream development). These biases then impact other regions resulting in biased atmospheric circulation across the NH. Indeed, in this study we confirm this via regional nudging experiments within the Norwegian Earth System Model. Namely, nudged horizontal winds over the North Pacific can improve Rossby wave statistics and thereby atmospheric circulation over Eurasia (i.e., upstream). However, nudging over the North Atlantic has little effect on boreal summer atmospheric circulation. This implies that improving biases over the North Pacific is crucial for a better representation of modelled boreal summer circulation over Eurasia.

KEY WORDS

blocking events, climate model bias, jet stream, nudging, Rossby waves, summer climate

1 | INTRODUCTION

Climate models exhibit biases in simulating many aspects of the mean climate and variability of the midlatitudes

This work reflects the analysis and views of the author Lina Boljka. No reader should interpret this work to present the views of any third party. Assumptions, opinions, views and estimates constitute the author's judgement as of the date given and are subject to change without notice and without duty to update.

(e.g., Harvey et al., 2020; Priestley et al., 2020, 2023; Simpson et al., 2020). In boreal summer, typical model biases include weaker storm tracks and poleward-shifted jet streams across the Northern Hemisphere (NH), both of which are especially pronounced in atmosphere-only configurations of climate models (for an intercomparison of atmosphere-only climate models, see Figure S1a,b). Among the factors that may contribute to such circulation biases are poor representation of atmosphere–ocean/land/ice exchange, land and sea surface temperature

This is an open access article under the terms of the [Creative Commons Attribution](#) License, which permits use, distribution and reproduction in any medium, provided the original work is properly cited.

© 2024 The Author(s). *Atmospheric Science Letters* published by John Wiley & Sons Ltd on behalf of Royal Meteorological Society.

(SST), diabatic processes, topography, teleconnections and other nonlinear processes in the climate system, as well as inadequate model resolution (Athanasiadis et al., 2022; Bony et al., 2015; Luo, 2005; Nakamura et al., 2010; Omrani et al., 2019; Seneviratne et al., 2010; Shaw et al., 2016; Steinfeld & Pfahl, 2019; Swanson, 2002; Wang et al., 2023).

In general, meridionally shifted jet streams may be linked to biases in temperature gradients (over land and sea) and the related energy available (directly) via thermal wind balance or (indirectly) via interactions with Rossby waves (e.g., positive baroclinic feedback; Robinson, 2000). Rossby waves are large-scale waves that help shape the general circulation of the atmosphere (and ocean) (e.g., Holton, 2004; Hoskins et al., 1983), but whose characteristics also depend on the mean strength and position of the jet stream (background zonal flow; \bar{u}). For example, Rossby wave phase speed (c) is (e.g., Holton, 2004)

$$c = \bar{u} - \beta / (k^2 + l^2), \quad (1)$$

where β is the meridional gradient of planetary vorticity, k is the zonal wavenumber and l is the meridional wavenumber. Equation (1) implies that if the background zonal flow is weak ($\bar{u} \rightarrow 0$) or the waves are long enough (k small), Rossby waves can propagate westward ($-\beta / (k^2 + l^2) < 0$) against the eastward mean flow ($\bar{u} > 0$). Shorter waves (k large) generally propagate eastward with the mean flow ($\bar{u} > 0$ dominates) and can affect regions downstream (e.g., via downstream seeding/development; Chang, 1993, 1999; Chang & Yu, 1999). Additionally, the jet stream affects the meridional propagation of Rossby waves and thereby wave-breaking and dissipation (Barnes & Hartmann, 2010; Hoskins & Ambrizzi, 1993). This in turn can affect atmospheric blocking events (e.g., Weijenborg et al., 2012), persistent high-pressure weather patterns characterized by a reversal of geopotential gradients (Kautz et al., 2022; Lupo, 2021), whose frequency is typically underestimated in climate models (Figure S1d; Davini & D'Andrea, 2020; Masato et al., 2013; Simpson et al., 2020).

Biases in the jet streams and Rossby waves have consequences not only for the upper-tropospheric circulation but also for surface climate (Luo et al., 2022). In NH summer, Rossby waves of all scales are important and interactions between synoptic scale waves and the large-scale flow have been shown to play a key role in producing persistent warm and dry events, such as those linked to heatwaves and droughts (Coumou et al., 2014; Kornhuber et al., 2017; Mann et al., 2017; Petoukhov et al., 2013; Pyrina et al., 2024). This means that the

erroneous representation of Rossby waves may also feedback onto the near-surface temperature gradients that set the large-scale atmospheric circulation.

The main goal of this study is to assess the potential role of biases in jet streams over the North Pacific and North Atlantic storm track regions in setting large-scale flow conditions over the NH continents. The storm tracks are preferred locations for the generation of Rossby waves, and their propagation away from these source regions produces remote effects both upstream and downstream. However, the wave propagation in models will be influenced by the poleward bias in the summer jet streams (Figure S1a,b). To assess the remote impacts of the jet biases on the atmospheric flow over the continents, we perform nudging experiments where winds in the storm track regions are corrected towards the observed climatology.

The study is structured as follows. Section 2 describes the model experiments, data and methods, Section 3 shows the results and discussion/conclusions are presented in Section 4.

2 | DATA AND METHODS

2.1 | Model experiments and data

We use the atmospheric component of the Norwegian Earth System Model (Selander et al., 2020) version 2.2 (NorESM2.2), which is based on the Community Atmosphere Model version 6 (CAM6) (Bogenschutz et al., 2018; Danabasoglu et al., 2020), with prescribed sea-surface temperature (SST). The model is run at medium resolution: $1.25^\circ \times 0.9424^\circ$ in the horizontal with 32 vertical levels. This model version allows a straightforward implementation of regional nudging, which we exploit to perform a number of experiments, all driven by monthly mean historical SSTs and external forcing over the period 1979–2013. We use ERA5 reanalysis (Hersbach et al., 2020), which is provided by the European Centre for Medium-Range Weather Forecasts, as the target data for nudging experiments (see also Equation 2).

The main experiments are: (1) control, that is, no nudging (CTL); (2) regional nudging of zonal and meridional winds to ERA5 reanalysis over the North Pacific region (Pacific nudging; Figure 1a); and (3) regional nudging of zonal and meridional winds to ERA5 reanalysis over the North Atlantic region (Atlantic nudging; Figure 1b). The model experiments are run for 35 years (1979–2013) of which the first year is taken as a spin-up period and the rest are analysed.

The regional nudging is achieved by relaxing the simulated wind field towards the ERA5 wind field (both the

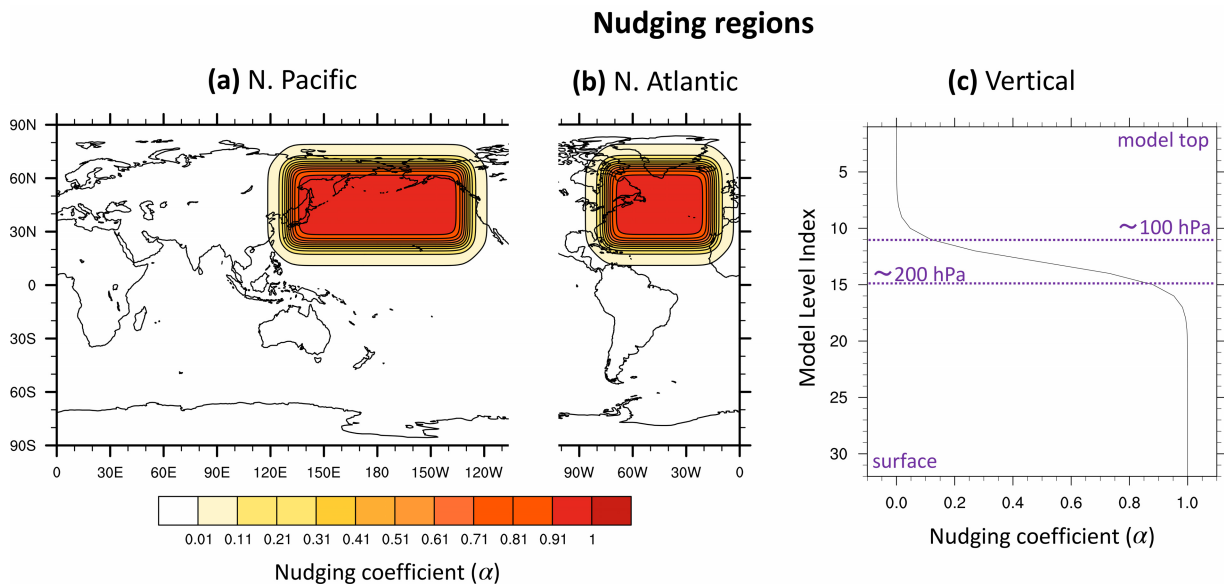


FIGURE 1 Nudging coefficient α (see Equations 3 and 4) for (a) Pacific nudging experiment, (b) Atlantic nudging experiment and (c) vertical extent of nudging in both experiments.

variability and mean state) in the troposphere only (Figure 1c). In practice, the nudging is implemented as a relaxation tendency between the instantaneous model state and a target state

$$F_{\text{nudge}} = \frac{\alpha}{\Delta t_{\text{nudge}}} (S_{\text{target}} - S_{\text{model}}), \quad (2)$$

where S is one of the variables we would like to nudge (zonal or meridional wind), α is a normalized strength coefficient ($\in [0,1]$) and Δt_{nudge} is the relaxation time scale (6 h). ERA5 data is provided to the model every 6 h and linearly interpolated for the time steps in between.

The nudging region is specified via a nudging window, where α increases from 0 (no nudging) to 1 (full strength nudging) both horizontally and vertically (Figure 1). The Pacific nudging region (Figure 1a,c) is specified as:

$$\alpha = \begin{cases} 1 & ; \\ & \phi \in [27.5, 62.5]^\circ, \lambda \in [135, 225]^\circ, \text{lvl} \geq 15 \\ & \tanh \text{decrease from 1 to 0} \\ & ; \\ & \text{transition zone} \\ 0 & ; \\ & \phi \lesssim 12.5^\circ \text{ or } \phi \gtrsim 77.5^\circ, \\ & \lambda \lesssim 115^\circ \text{ or } \lambda \gtrsim 245^\circ, \text{lvl} \leq 11, \end{cases} \quad (3)$$

where ϕ is latitude (in degrees north), λ is longitude (in degrees east) and lvl is model level counter (with level 1 at the top of the atmosphere and level 33 at the surface; lvl = 11 corresponds to ~ 100 hPa, lvl = 15 corresponds to ~ 200 hPa).

Similarly, the Atlantic nudging region (Figure 1b,c) is:

$$\alpha = \begin{cases} 1 & ; \\ & \phi \in [27.5, 62.5]^\circ, \lambda \in [290, 340]^\circ, \text{lvl} \geq 15 \\ & \tanh \text{decrease from 1 to 0} \\ & ; \\ & \text{transition zone} \\ 0 & ; \\ & \phi \lesssim 12.5^\circ \text{ or } \phi \gtrsim 77.5^\circ, \\ & \lambda \lesssim 270^\circ \text{ or } \lambda \gtrsim 0^\circ, \text{lvl} \leq 11. \end{cases} \quad (4)$$

These regions are defined such that the horizontal winds are strongly nudged over the midlatitude oceans, leaving winds over the continents, the Tropics and the Poles largely untouched (Figure 1). The flow in other regions will adjust to the ‘corrected’ wind field, as will other atmospheric variables (importantly, temperature), raising the possibility of unwanted spurious circulation responses. To check this, we have performed four sensitivity experiments based on the Pacific nudging experiment (2): (i) as in (2) but in a smaller region; (ii) as in

(2) but nudging temperature along with the wind field; (iii) so-called ‘anomaly nudging’ where the wind field is relaxed towards the model’s climatology with ERA5 variability superimposed; and (iv) ‘online’ bias correction where the climatological seasonal cycle (by day-of-year) of nudging tendencies from (2) is applied as an additional forcing term to the relevant momentum equations. The latter means that the difference between ERA5 and control run is prescribed in the form of mean nudging tendencies, which then acts as an effective ‘online’ bias correction of the model’s mean state.

Experiment (i) yields similar results to the Pacific nudging experiment (not shown). Experiment (ii) produces slightly stronger corrections to the flow within the nudging region itself due to the additional temperature constraint, but yields similar results to the Pacific nudging experiment elsewhere (not shown). Thus, wind nudging alone is a good approach for the purposes of this study, as has also been shown by others (Figure S10; Zhang et al., 2014). Experiments (iii) and (iv) are brought into the discussion where appropriate (Section 4; Figure S9) to help clarify the role of mean state versus variability biases. Note that our focus is not the sensitivity of the model to nudging, but rather on whether ‘correcting’ the tropospheric circulation in one region can improve the mean state and variability elsewhere.

The NorESM2.2 experiments are compared to the ERA5 reanalysis (Hersbach et al., 2020). For broader context, we also show selected results using atmosphere-only (AMIP) model simulations from the Coupled Model Intercomparison Project Phase 6 (CMIP6; Eyring et al., 2016) in the supplement (Figure S1; Table S1). All data are analysed at 2.5° horizontal resolution and on specific pressure levels (see below) over the period 1980–2013 for consistency.

2.2 | Methods

We focus on summer season (June–July–August; JJA) averages using geopotential height (Z) at 500 and 250 hPa, zonal wind (u) at 850 and 250 hPa and meridional wind (v) at 250 hPa.

Rossby wave statistics are inferred from the root-mean-square (amplitude) of filtered daily-mean Z at 500 hPa (Lau, 1988). Using wavenumber filtering (via Fourier transform), waves are categorized as long (zonal wavenumber $k \leq 4$) or short ($k \geq 5$). A breakdown into stationary (climatological) and transient (after removing the smoothed (first four harmonics) daily seasonal cycle) components is performed, with the transient waves further filtered (5th order Butterworth, cut-off period of

12 days) to obtain low- and high-frequency components. Some results are presented in the form of lagged regression maps, where low-frequency Z at 250 hPa is regressed onto the reference timeseries from a specific region. Additionally, the Rossby wave source¹ (Sardeshmukh & Hoskins, 1988; Scaife et al., 2017) and horizontal components of the E-vector² (Hoskins et al., 1983) are computed to assess how the generation and propagation of Rossby wave trains (impact on the mean flow/jet streams) changes between experiments (for details see Figure S10).

Blocking frequency is computed as the number of blocking events per day. Blocking events are identified via the daily mean geopotential height gradient reversal at 500 hPa (Z_{500}) at each grid point between 35° N and 75° N (ϕ_0) and over 15 degrees of latitude (ϕ_N, ϕ_S) as (Cheung et al., 2023; Scherrer et al., 2006)

$$\text{GHGN}(\lambda, \phi_0, t) = \frac{Z_{500}(\lambda, \phi_N, t) - Z_{500}(\lambda, \phi_0, t)}{\phi_N - \phi_0} < -10 \text{ m/}^\circ\text{latitude}, \quad (5)$$

$$\text{GHGS}(\lambda, \phi_0, t) = \frac{Z_{500}(\lambda, \phi_0, t) - Z_{500}(\lambda, \phi_S, t)}{\phi_S - \phi_0} > 0 \text{ m/}^\circ\text{latitude}, \quad (6)$$

with $\phi_0 \in [35, 75]^\circ$ N, $\phi_N = \phi_0 + 15^\circ$ N, $\phi_S = \phi_0 - 15^\circ$ N. Additionally, the blocked area must be at least 10^6 km^2 in spatial extent, and blocking should persist for at least 4 days to be classified as an event.

3 | RESULTS

3.1 | Mean state

First, we assess the response of the boreal summer circulation to regional nudging. In reanalysis, NH summer is characterized by a rather zonally symmetric mean state (Figure 2a showing Z at 500 hPa), consistent with weakly tilted jet streams in both storm track regions (Figure 2e,i). There is also a subtropical jet stream across central Eurasia (Figure 2i) and a weaker subpolar jet stream across high-latitude Eurasia (Figure 2e).

The control experiment exhibits substantial biases in these fields. Most notable are the poleward-shifted jet streams, evident at lower (Figure 2f) and upper (Figure 2j) levels. Consistent with the biases in zonal winds are biases in mid-tropospheric geopotential height (Figure 2b), namely overly low Z in the polar regions and overly high Z in the midlatitudes. These biases are broadly consistent with biases in other AMIP simulations (Figure S1a–c) and in coupled climate models

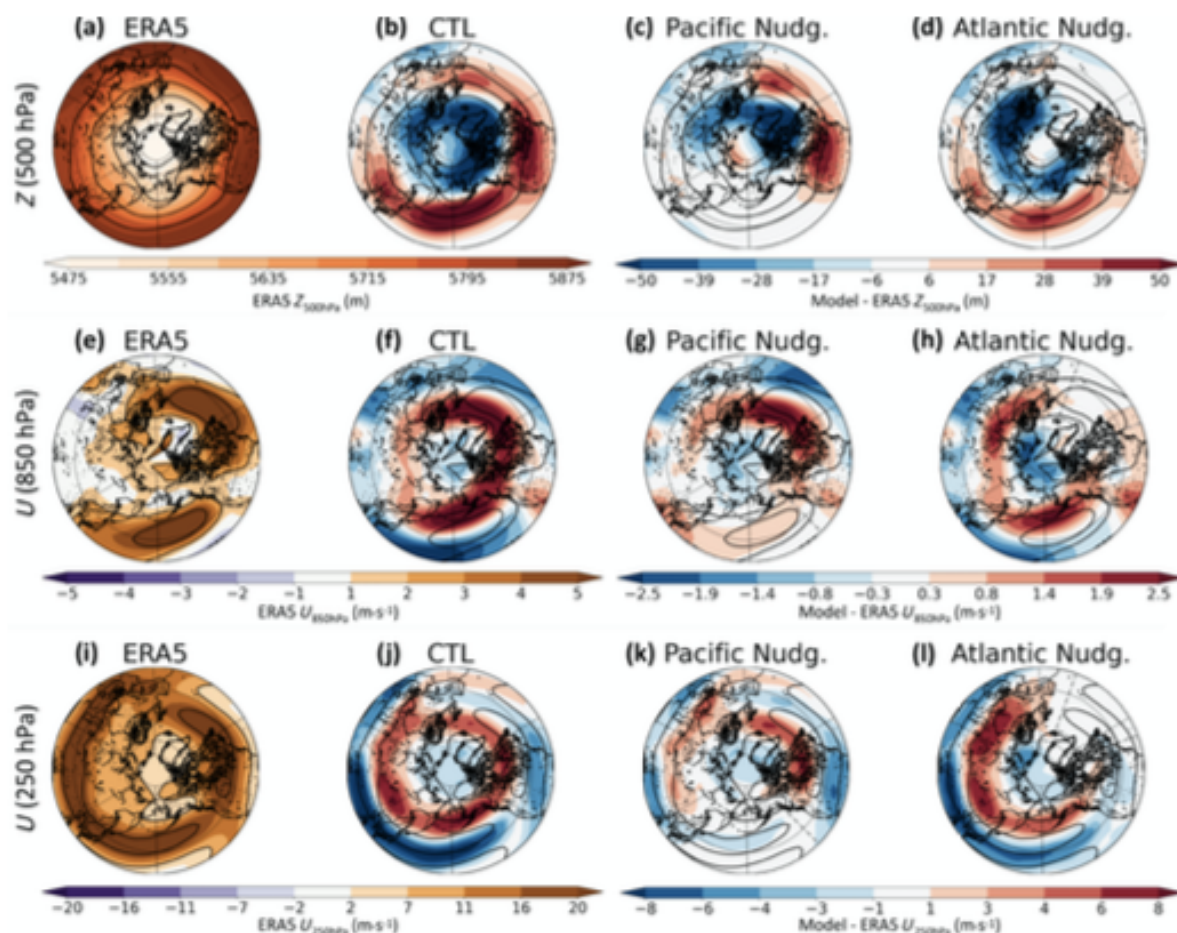


FIGURE 2 Climatology of geopotential height Z at 500 hPa (in m; top row), zonal wind U at 850 hPa (in m s^{-1} ; middle row) and at 250 hPa (in m s^{-1} ; bottom row) for JJA. ERA5 climatology is shown in the left-most column (a, e, i). The other columns represent the difference between model experiments and ERA5 for the (b, f, j) control (CTL) experiment, (c, g, k) Pacific nudging experiment and (d, h, l) Atlantic nudging experiment. Contours in all panels represent selected contours of the respective ERA5 climatology. Left colour bars are for ERAS climatology, right colour bars are for the model bias relative to ERA5.

(e.g., Harvey et al., 2020; Priestley et al., 2023; Simpson et al., 2020).

The Pacific (Figure 2c,g,k) and Atlantic (Figure 2d,h,l) nudging experiments show improved mean states in their respective nudging regions (by design), but the remote responses are quite different. Atlantic nudging (Figure 2d,h,l) slightly reduces the mean-state biases over the Pacific, but slightly worsens the mean-state bias over Eurasia. On the other hand, Pacific nudging (Figure 2c,g,k) reduces biases in the Eurasian jet stream (Figure 2k), but does not lead to improvements elsewhere. In both experiments, the main improvements are directly *upstream* from the nudging region. To help understand this somewhat counterintuitive result, we examine the response of Rossby waves to the nudging, in particular the

differences between long and short waves, which can differ in their zonal propagation directions (see Introduction).

3.2 | Long and short Rossby waves

As mentioned in the introduction, a meridionally shifted jet stream can affect Rossby waves. A poleward bias in the jet stream strengthens the mean westerly flow (more positive \bar{u}) at higher latitudes. This can hinder westward (or promote eastward) propagation of long waves ($k \leq 4$) at higher latitudes and promote westward (or hinder eastward) propagation at lower latitudes, resulting in biases both upstream and downstream of the wave-origin region.

Long Waves ($k \leq 4$)

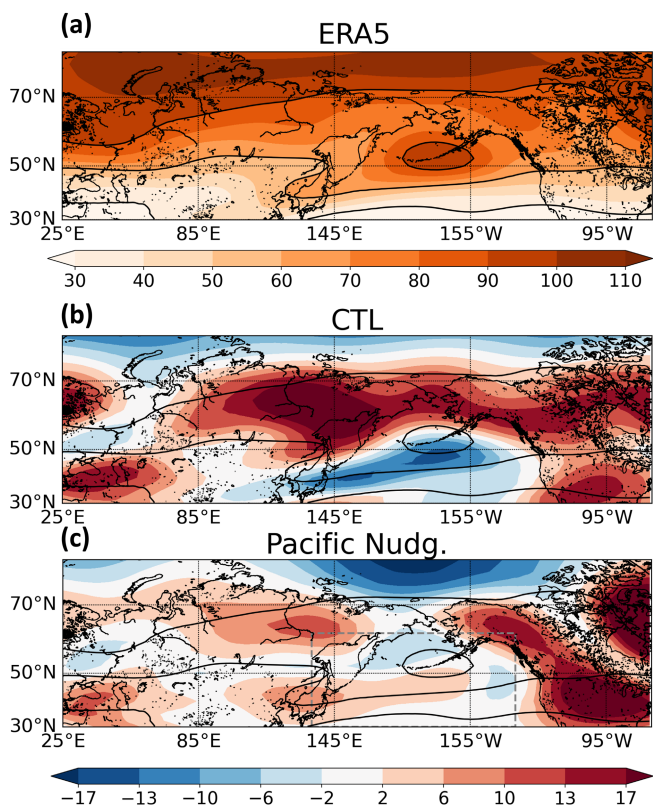


FIGURE 3 Root-mean-square of Z at 500 hPa for long waves ($k \leq 4$). (a) ERA5 climatology, (b) difference in climatology between CTL experiment and ERA5 and (c) difference in climatology between Pacific nudging experiment and ERA5. Contours in all panels represent select contours of ERA5 climatology from (a).

Indeed, there are substantial errors (relative to ERA5; Figures 3a, S2a, S3a and S4a) in long wave statistics in the control experiment (Figures 3b and S3b), dominated by the transient component (Figures S2b and S4b). Focusing on the Pacific, the long wave activity is shifted poleward, consistent with the poleward bias of the Pacific jet stream (positive baroclinic feedback; Robinson, 2000), but there are also associated biases upstream and downstream. When nudging is switched on (Figures 3c and S2c), local biases in long wave statistics vanish (by design) and are reduced upstream. However, effects downstream are less straightforward: long wave statistics worsen overall (Figure 3c) even though transient biases are reduced (Figure S2c), suggesting that the stationary component dominates in this region. Similar results for long waves are found in the Atlantic nudging experiment, though the upstream improvements of transient long waves are much smaller and downstream improvements of stationary waves are better (Figures S3c and S4c).

Figure 4 confirms that Pacific nudging improves the westward propagation of long waves (assessed via low-

frequency Z at 250 hPa) at higher latitudes. With nudging, the Pacific jet (Figure 2g,k) is further equatorward (like in ERA5 relative to CTL (Figure 2f,j), and the weaker high-latitude background flow permits ‘faster’ westward wave propagation (Equation 1). Indeed, long-wave packets originating north of the Aleutian Islands are estimated to propagate westward across Eurasia at around $2 \text{ m}\cdot\text{s}^{-1}$ in CTL (Figure 4, right column and Table S2) and $5 \text{ m}\cdot\text{s}^{-1}$ with Pacific nudging (middle column), with the latter comparing better to the $6.5 \text{ m}\cdot\text{s}^{-1}$ propagation speed in ERA5 (left column). We find consistent results at lower latitudes, where nudging strengthens the westerlies and slows westward wave propagation (Figure S5).

The above results suggest that a better representation of horizontal winds improves the representation of long waves in and upstream of the nudged region (Figure 3c). This improves momentum fluxes of Rossby waves (compare Figure S10f,j with Figure S10g,k) that drive the mid-latitude jet streams. This in turn improves the Eurasian jet stream (Figure 2k) through wave-mean flow interactions (Hoskins et al., 1983; Figure S10e-l).

Short wave ($k \geq 5$) activity associated with the midlatitude storm tracks is also affected by a poleward-biased jet stream. Figure 5b shows that the control experiment exhibits weaker storm tracks than ERA5 (Figure 5a), consistent with typical storm track biases in atmosphere-only and coupled climate models (Priestley et al., 2020, 2023). The storm tracks are also poleward shifted compared to ERA5, especially in the Pacific.

Again focusing on the Pacific, nudging improves storm track intensity locally (by design) as well as downstream (Figure 5c), with both high- and low-frequency components contributing (Figure S6). However, the modulation of short waves downstream of the nudging region is weak, perhaps due in part to persistent long-wave biases over North America (Figure 3c). Consistent with little change in the short wave statistics further downstream, the jet stream bias over the Atlantic remains similar with Pacific nudging (Figure 2f,g,j,k). This may be because: (i) the jet bias over the Atlantic is smaller than over the Pacific in CTL (less room for improvement); or (ii) the Atlantic exhibits regime behaviour in summer (Rousi et al., 2022) just as in winter (Woollings et al., 2010), which is more difficult to change through mean-state nudging.

Similarly, we find a weak downstream influence in the Atlantic nudging experiment relative to the control experiment (Figure S7). However, the Atlantic experiment is somewhat more complicated as the high-frequency short waves are actually degraded downstream of the nudging region (over Eurasia) relative to the control experiment (Figure S8). This can explain the bias in

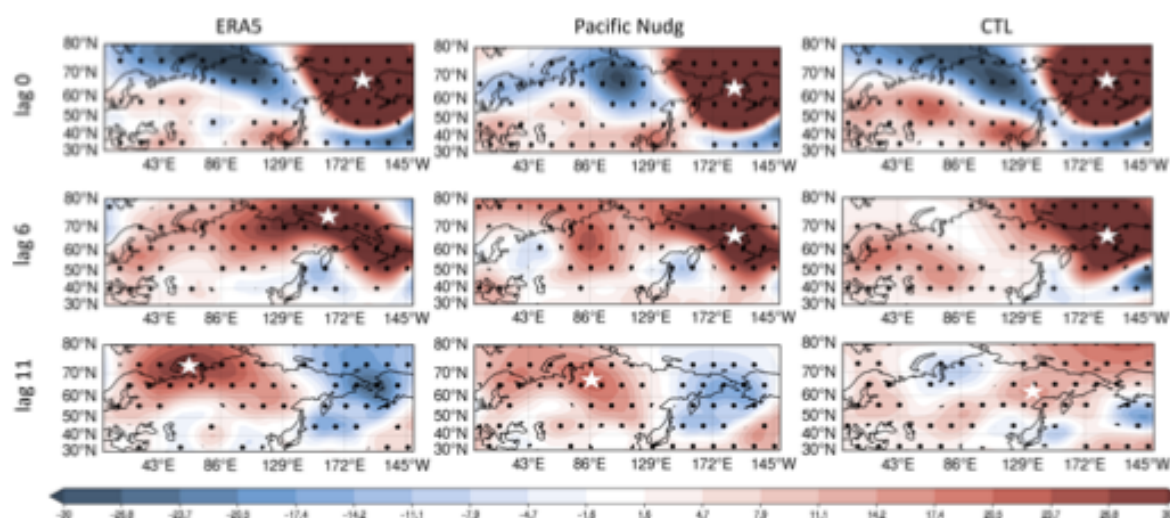


FIGURE 4 Lag-regression of low-frequency filtered Z at 250 hPa (in m) across the NH with the time series of the spatial average over 55° – 75° N and 170° E– 150° W (as an example). Results are shown for ERA5 (left column), Pacific nudging experiment (middle column) and control simulation (right column) at lags 0 (top row), 6 (middle row) and 11 (bottom row) days. Stippling denotes statistically significant values at 95% level. Stars roughly follow the centre of action of the anomalous positive Z anomalies that propagate westward (for visualization purposes). Here, anomalies in the control simulation (right column; zonal winds displaced poleward) move westward slower (they stall) than in ERA5 or in the Pacific nudging experiment (left and centre columns).

the Eurasian jet stream with Atlantic nudging (Figure 2h,l), and indicates issues in the downstream response of the atmospheric circulation to changes in the Atlantic variability and mean state. Reasons may again lie in the North Atlantic's regime behaviour (see above).

The results presented in this section suggest that improvements in mean state seen in the (Pacific) nudging experiments (Section 3.1) are mainly linked to westward propagating long waves, which interact with the mean flow upstream. However, eastward propagating short waves do not lead to circulation improvements downstream.

3.3 | Blocking frequency

Biases in jet position can also affect Rossby waves through factors linked to meridional propagation (Figure S10i-l). A poleward jet bias can inhibit poleward propagation of Rossby waves (e.g., Barnes et al., 2010; Barnes & Hartmann, 2010). Instead, they may remain (meridionally) trapped or propagate equatorward and dissipate (Figure S10j), reinforcing the poleward bias. Further, too little dissipation (wave-breaking) poleward of the jet can lead to underestimation of high-latitude atmospheric blocking events (Barnes & Hartmann, 2010; Weijenborg et al., 2012), as seen in the control experiment relative to ERA5 (Figure 6a,b). Additionally, note

that identification of blocking events (see Equations 5 and 6) depends on the representation of Z (Figure S1c; Simpson et al., 2020), which is also biased in the control experiment (Figure 2b).

These circulation biases are substantially reduced in the Pacific nudging experiment (Figures 2c,g,k and S10g, k), especially over Eurasia. Consistently, blocking frequency (Figure 6c) is improved (relative to the control experiment; Figure 6b) over high-latitude Eurasia. However, blocking does not improve in the Atlantic nudging experiment (Figure 6d), consistent with no improvement in other circulation metrics in this experiment (Figures 2d,h,l and S10h,l). Hence, improved blocking frequency with Pacific nudging may result from more realistic atmospheric circulation over Eurasia, with a properly placed jet that allows space for waves to propagate polewards, break and promote blocking (Figure 6c).

4 | DISCUSSION AND CONCLUSION

This study has examined the response of the boreal summer climate to regional nudging of horizontal winds over the North Atlantic and North Pacific basins. Overall, we find the largest bias reductions in circulation metrics (jet stream, Rossby waves, blocking frequency) over Eurasia in the Pacific nudging experiment (Figures 2c,g,k, 3c, 5c

and 6c). A possible explanation involves improvements in westward propagating long waves (Figure 3c), which then feedback on the mean flow over Eurasia, shifting the Eurasian subtropical jet stream equatorward to a

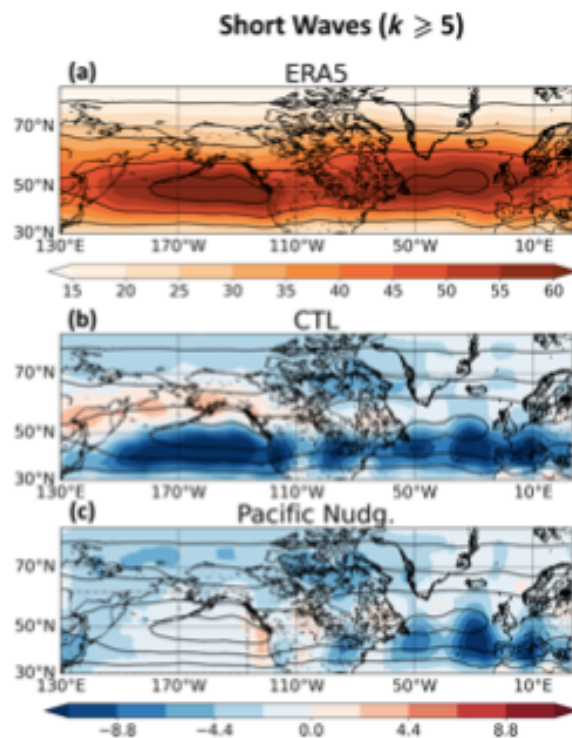


FIGURE 5 Root-mean-square of Z at 500 hPa for short waves ($k \geq 5$). (a) ERA5 climatology, (b) difference in climatology between CTL experiment and ERA5 and (c) difference in climatology between Pacific nudging experiment and ERA5. Contours in all panels represent select contours of ERA5 climatology from (a). Note that short waves are dominated by their transient component (not shown).

more realistic latitude. The importance of Rossby waves for reducing biases in boreal summer climate was noted in Luo et al. (2022); other processes, including diabatic heating, may also play a role (Joshi & Zhang, 2023). Consistent with improvements in atmospheric circulation, there is a reduction in blocking frequency bias linked to improvements in geopotential height (Simpson et al., 2020) and jet stream latitude (Barnes et al., 2010; Weijenborg et al., 2012). Interestingly, we find much weaker improvements in the atmospheric circulation upstream and (especially) downstream in the Atlantic nudging experiment (Figures 2d,h,l, S3c, S7c and 6d). Similarly, there are no clear improvements from nudging during boreal winter where biases in AMIP models are already small (not shown).

To clarify whether correcting biases in the mean state or in the variability is more important for improving boreal summer circulation, we performed additional experiments (Section 2.1): (iii) Pacific anomaly nudging and (iv) Pacific climatological bias-correction. Experiment (iii) shows no improvement in circulation over Eurasia (Figure S9, left column) relative to the control experiment (Figures 2f,j and 6b), whereas experiment (iv) shows reduced biases (compare Figure S9, right column and Figures 2f,j and 6b). The bias-corrected circulation is similar to the Pacific nudging experiment, confirming that it is the climatological mean-state bias of the horizontal winds (jet stream) that affects the Eurasian summer climate and not a correction (nudging) of anomalies (variability). Given that the poleward bias of the summer jet streams is a common feature of many climate models (Figure S1a,b; see also, e.g., Harvey et al., 2020; Simpson et al., 2020), these results may be generalizable beyond the NorESM2.2 (CAM6) model used here.

Biases in Eurasian climate can originate from other factors as well. For example, Priestley et al. (2023) suggest

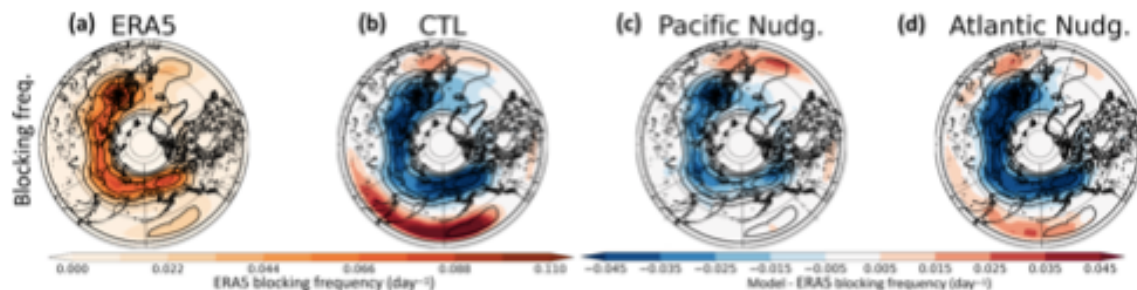


FIGURE 6 Climatology of blocking frequency (in day^{-1}) for JJA. ERA5 climatology is shown in panel (a). The other panels represent the difference between model experiments and ERA5 for (b) control (CTL) experiment, (c) Pacific nudging experiment and (d) Atlantic nudging experiment. Contours in all panels represent selected contours of the ERA5 climatology from (a). Left colour bars are for ERA5 climatology, right colour bars are for the model bias relative to ERA5.

that the overheated central Asian landmass contributes to a poleward-shifted jet stream over Eurasia, as well as to weakening of temperature gradients equatorward of the jet, which results in a weaker storm track. Thus, the atmospheric circulation over Eurasia and the North Pacific are intrinsically linked, with a two-way interaction between the regions ultimately setting the summer circulation biases in climate models. We have shown that the North Pacific atmospheric circulation plays an important role for boreal summer climate and highlighted importance of long-wave signals upstream of storm-track regions. Identifying the causes for these biases should be a subject of further research.

Open research: NorESM2.2 model code is freely available on github (<https://github.com/NorESMhub/NorESM/tree/noresm2.2>) and details about using this model version as well as regional nudging implementation can be found here: <https://noresm22-nudging-regional.readthedocs.io/en/latest/index.html>. ERA5 data are available through <https://cds.climate.copernicus.eu/> (Hersbach et al., 2020). CMIP6 model data are accessible through <https://esgf-node.llnl.gov/search/cmip6/> (Eyring et al., 2016).

AUTHOR CONTRIBUTIONS

Lina Boljka: Methodology; conceptualization; investigation; funding acquisition; writing – original draft; validation; visualization; writing – review and editing; formal analysis; data curation. **Ingo Bethke:** Conceptualization; investigation; funding acquisition; methodology; data curation; writing – review and editing; software. **Dandan Tao:** Conceptualization; writing – review and editing; funding acquisition; methodology; software. **Camille Li:** Conceptualization; writing – review and editing; methodology.

ACKNOWLEDGEMENTS

This work was funded by Bjerknes Centre Fast Track Initiative and Trond Mohn Foundation (project BCPU, grant number BFS2018TMT01). IB is additionally supported by the Research Council of Norway (Grant 309562; Climate Futures). This work also used Norwegian Research Infrastructure Services (NRIS), that is, NIRD/Sigma2 and Betzy/Sigma2 (project NS9039K, NN9039K). We thank Will Chapman and Stefan Sobolowski for helpful discussions, as well as Ho-Nam Cheung for kindly sharing the blocking code.

FUNDING INFORMATION

This study was supported by the Bjerknes Centre Fast Track Initiative; Trond Mohn Foundation (project BCPU), grant number BFS2018TMT01; Research Council of Norway (Grant 309562; Climate Futures).

CONFLICT OF INTEREST STATEMENT

The authors declare no conflicts of interest.

DATA AVAILABILITY STATEMENT

The data that support the findings of this study are available from the corresponding author upon reasonable request.

ORCID

Lina Boljka  <https://orcid.org/0000-0003-4197-9350>

ENDNOTES

¹ Rossby wave source = $-\nabla \cdot (\mathbf{v}_\zeta \zeta)$, where ζ is absolute vorticity, \mathbf{v}_ζ is the divergent component of horizontal wind and ∇ -operator is computed in spherical coordinates.

² E-vector = $(v^2 - u'^2, -u'v')$ where u and v are zonal and meridional winds, and prime ('') denotes perturbation from smooth seasonal cycle.

REFERENCES

- Athanasiadis, P.J., Ogawa, F., Omrani, N.-E., Keenlyside, N., Schiemann, R., Baker, A.J. et al. (2022) Mitigating climate biases in the midlatitude North Atlantic by increasing model resolution: SST gradients and their relation to blocking and the jet. *Journal of Climate*, 35(21), 3385–3406. Available from: <https://doi.org/10.1175/JCLI-D-21-0515.1>
- Barnes, E.A. & Hartmann, D.L. (2010) Influence of eddy-driven jet latitude on North Atlantic jet persistence and blocking frequency in cmip3 integrations. *Geophysical Research Letters*, 37(23), L23802. Available from: <https://doi.org/10.1029/2010GL045700>
- Barnes, E.A., Hartmann, D.L., Frierson, D.M.W. & Kidston, J. (2010) Effect of latitude on the persistence of eddy-driven jets. *Geophysical Research Letters*, 37(11), L11804. Available from: <https://doi.org/10.1029/2010GL043199>
- Bogenschutz, P.A., Gettelman, A., Hannay, C., Larson, V.E., Neale, R.B., Craig, C. et al. (2018) The path to cam6: coupled simulations with cam5.4 and cam5.5. *Geoscientific Model Development*, 11(1), 235–255. Available from: <https://doi.org/10.5194/gmd-11-235-2018>
- Bony, S., Stevens, B., Frierson, D.M.W., Jakob, C., Kageyama, M., Pincus, R. et al. (2015) Clouds, circulation and climate sensitivity. *Nature Geoscience*, 8(4), 261–268. Available from: <https://doi.org/10.1038/ngeo2398>
- Chang, E.K.M. & Yu, D.B. (1999) Characteristics of wave packets in the upper troposphere. Part I: Northern Hemisphere winter. *Journal of the Atmospheric Sciences*, 56, 1708–1728.
- Chang, E.K.M. (1993) Downstream development of baroclinic waves as inferred from regression analysis. *Journal of the Atmospheric Sciences*, 50, 2038–2053.
- Chang, E.K.M. (1999) Characteristics of wave packets in the upper troposphere. Part II: seasonal and hemispheric variations. *Journal of the Atmospheric Sciences*, 56(11), 1729–1747.
- Cheung, H.-N., Omrani, N.-E., Ogawa, F., Keenlyside, N., Nakamura, H. & Zhou, W. (2023) Pacific oceanic front amplifies the impact of Atlantic oceanic front on North Atlantic blocking. *npj Climate and Atmospheric Science*, 6(1), 61. Available from: <https://doi.org/10.1038/s41612-023-00370-x>

- Coumou, D., Petoukhov, V., Rahmstorf, S., Petri, S. & Schellnhuber, H.J. (2014) Quasi-resonant circulation regimes and hemispheric synchronization of extreme weather in boreal summer. *Proceedings of the National Academy of Sciences*, 111(34), 12331–12336. Available from: <https://doi.org/10.1073/pnas.1412797111>
- Danabasoglu, G., Lamarque, J.-F., Bacmeister, J., Bailey, D.A., DuVivier, A.K., Edwards, J. et al. (2020) The community earth system model version 2 (cesm2). *Journal of Advances in Modeling Earth Systems*, 12(2), e2019MS001916. Available from: <https://doi.org/10.1029/2019MS001916>
- Davini, P. & D'Andrea, F. (2020) From CMIP3 to CMIP6: Northern Hemisphere atmospheric blocking simulation in present and future climate. *Journal of Climate*, 33(23), 10021–10038. Available from: <https://doi.org/10.1175/JCLI-D-19-0862.1>
- Eyring, V., Bony, S., Meehl, G.A., Senior, C.A., Stevens, B., Stouffer, R.J. et al. (2016) Overview of the coupled model intercomparison project phase 6 (CMIP6) experimental design and organization. *Geoscientific Model Development*, 9(5), 1937–1958. Available from: <https://doi.org/10.5194/gmd-9-1937-2016>
- Harvey, B.J., Cook, P., Shaffrey, L.C. & Schiemann, R. (2020) The response of the Northern Hemisphere storm tracks and jet streams to climate change in the CMIP3, CMIP5, and CMIP6 climate models. *Journal of Geophysical Research: Atmospheres*, 125(23), e2020JD032701. Available from: <https://doi.org/10.1029/2020JD032701>
- Hersbach, H., Bell, B., Berrisford, P., Hirahara, S., Horányi, A., Muñoz-Sabater, J. et al. (2020) The era5 global reanalysis. *Quarterly Journal of the Royal Meteorological Society*, 146(730), 1999–2049. Available from: <https://doi.org/10.1002/qj.3803>
- Holton, J.R. (2004) *An introduction to dynamic meteorology*, 4th edition. London: Elsevier Academic Press.
- Hoskins, B.J., James, I.N. & White, G.H. (1983) The shape, propagation and mean-flow interaction of large-scale weather systems. *Journal of the Atmospheric Sciences*, 40, 1595–1612.
- Hoskins, B.J. & Ambrizzi, T. (1993) Rossby wave propagation on a realistic longitudinally varying flow. *Journal of the Atmospheric Sciences*, 50, 1661–1671.
- Joshi, R. & Zhang, R. (2023) Impacts of the North Atlantic biases on the upper troposphere/lower stratosphere over the extratropical north pacific. *npj Climate and Atmospheric Science*, 6(1), 151. Available from: <https://doi.org/10.1038/s41612-023-00482-4>
- Kautz, L.-A., Martius, O., Pfahl, S., Pinto, J.G., Ramos, A.M., Sousa, P.M. et al. (2022) Atmospheric blocking and weather extremes over the Euro-Atlantic sector—a review. *Weather and Climate Dynamics*, 3(1), 305–336. Available from: <https://doi.org/10.5194/wcd-3-305-2022>
- Kornhuber, K., Petoukhov, V., Petri, S., Rahmstorf, S. & Coumou, D. (2017) Evidence for wave resonance as a key mechanism for generating high-amplitude quasi-stationary waves in boreal summer. *Climate Dynamics*, 49(5), 1961–1979. Available from: <https://doi.org/10.1007/s00382-016-3399-6>
- Lau, N.-C. (1988) Variability of the observed midlatitude storm tracks in relation to low-frequency changes in the circulation pattern. *Journal of the Atmospheric Sciences*, 45, 2718–2743. Available from: [https://doi.org/10.1175/1520-0469\(1988\)045<2718:VOTOMS>2.0.CO;2](https://doi.org/10.1175/1520-0469(1988)045<2718:VOTOMS>2.0.CO;2)
- Luo, D. (2005) A barotropic envelope Rossby soliton model for block-eddy interaction. Part I: effect of topography. *Journal of the Atmospheric Sciences*, 62(1), 5–21. Available from: <https://doi.org/10.1175/1186.1>
- Luo, F., Selten, F., Wehrli, K., Kornhuber, K., Le Sager, P., May, W. et al. (2022) Summertime Rossby waves in climate models: substantial biases in surface imprint associated with small biases in upper-level circulation. *Weather and Climate Dynamics*, 3(3), 905–935. Available from: <https://doi.org/10.5194/wcd-3-905-2022>
- Lupo, A.R. (2021) Atmospheric blocking events: a review. *Annals of the New York Academy of Sciences*, 1504(1), 5–24. Available from: <https://doi.org/10.1111/nyas.14557>
- Mann, M.E., Rahmstorf, S., Kornhuber, K., Steinman, B.A., Miller, S.K. & Coumou, D. (2017) Influence of anthropogenic climate change on planetary wave resonance and extreme weather events. *Scientific Reports*, 7(1), 45242. Available from: <https://doi.org/10.1038/srep45242>
- Masato, G., Hoskins, B.J. & Woollings, T. (2013) Winter and summer Northern Hemisphere blocking in cmip5 models. *Journal of Climate*, 26(18), 7044–7059. Available from: <https://doi.org/10.1175/JCLI-D-12-00466.1>
- Nakamura, H., Takafumi Miyasaka, Y., Kosaka, K.T. & Honda, M. (2010) *Northern Hemisphere extratropical tropospheric planetary waves and their low-frequency variability: their vertical structure and interaction with transient eddies and surface thermal contrasts*. Washington, DC: American Geophysical Union (AGU), pp. 149–179. Available from: <https://doi.org/10.1029/2008GM000789>
- Omrani, N.-E., Ogawa, F., Nakamura, H., Keenlyside, N., Lubis, S.W. & Matthes, K. (2019) Key role of the ocean western boundary currents in shaping the Northern Hemisphere climate. *Scientific Reports*, 9(1), 3014. Available from: <https://doi.org/10.1038/s41598-019-39392-y>
- Petoukhov, V., Rahmstorf, S., Petri, S. & Schellnhuber, H.J. (2013) Quasiresonant amplification of planetary waves and recent Northern Hemisphere weather extremes. *Proceedings of the National Academy of Sciences*, 110(14), 5336–5341. Available from: <https://doi.org/10.1073/pnas.1222000110>
- Priestley, M.D.K., Ackerley, D., Catto, J.L. & Hodges, K.I. (2023) Drivers of biases in the CMIP6 extratropical storm tracks. Part I: Northern Hemisphere. *Journal of Climate*, 36(5), 1451–1467. Available from: <https://doi.org/10.1175/JCLI-D-20-0976.1>
- Priestley, M.D.K., Ackerley, D., Catto, J.L., Hodges, K.I., McDonald, R.E. & Lee, R.W. (2020) An overview of the extra-tropical storm tracks in CMIP6 historical simulations. *Journal of Climate*, 33(15), 6315–6343. Available from: <https://doi.org/10.1175/JCLI-D-19-0928.1>
- Pyrina, M., Wicker, W., de Vries, A.J., Fragkoulidis, G. & Domeisen, D.I.V. (2024) Rossby wave packets driving concurrent and non-concurrent heatwaves in the Northern and Southern Hemisphere mid-latitudes. *EGUSphere*, 2024, 1–44. Available from: <https://doi.org/10.5194/egusphere-2023-3088>
- Robinson, W.A. (2000) A baroclinic mechanism for the eddy feedback on the zonal index. *Journal of the Atmospheric Sciences*, 57, 415–422.
- Rousi, E., Kornhuber, K., Beobide-Arsuaga, G., Luo, F. & Coumou, D. (2022) Accelerated western European heatwave trends linked to more-persistent double jets over Eurasia. *Nature Communications*, 13(1), 3851. Available from: <https://doi.org/10.1038/s41467-022-31432-y>

- Sardeshmukh, P.D. & Hoskins, B.J. (1988) The generation of global rotational flow by steady idealized Tropical divergence. *Journal of the Atmospheric Sciences*, 45, 1228–1251. Available from: [https://doi.org/10.1175/1520-0469\(1988\)045<1228:TGOGRF>2.0.CO;2](https://doi.org/10.1175/1520-0469(1988)045<1228:TGOGRF>2.0.CO;2)
- Scaife, A.A., Comer, R.E., Dunstone, N.J., Knight, J.R., Smith, D.M., MacLachlan, C. et al. (2017) Tropical rainfall, Rossby waves and regional winter climate predictions. *Quarterly Journal of the Royal Meteorological Society*, 143(702), 1–11. Available from: <https://doi.org/10.1002/qj.2910>
- Scherrer, S.C., Croci-Maspoli, M., Schwierz, C. & Appenzeller, C. (2006) Two-dimensional indices of atmospheric blocking and their statistical relationship with winter climate patterns in the Euro-Atlantic region. *International Journal of Climatology*, 26(2), 233–249. Available from: <https://doi.org/10.1002/joc.1250>
- Seland, Ø., Bentsen, M., Olivé, D., Toniazzo, T., Gjermundsen, A., Graff, L.S. et al. (2020) Overview of the Norwegian earth system model (NorESM2) and key climate response of CMIP6 deck, historical, and scenario simulations. *Geoscientific Model Development*, 13(12), 6165–6200. Available from: <https://doi.org/10.5194/gmd-13-6165-2020>
- Seneviratne, S.I., Corti, T., Davin, E.L., Hirschi, M., Jaeger, E.B., Lehner, I. et al. (2010) Investigating soil moisture–climate interactions in a changing climate: a review. *Earth-Science Reviews*, 99(3), 125–161. Available from: <https://doi.org/10.1016/j.earscirev.2010.02.004>
- Shaw, T.A., Baldwin, M., Barnes, E.A., Caballero, R., Garfinkel, C.I., Hwang, Y.-T. et al. (2016) Storm track processes and the opposing influences of climate change. *Nature Geoscience*, 9, 656–664. Available from: <https://doi.org/10.1038/ngeo2783>
- Simpson, I.R., Bacmeister, J., Neale, R.B., Hannay, C., Gettelman, A., Garcia, R.R. et al. (2020) An evaluation of the large-scale atmospheric circulation and its variability in cesm2 and other cmip models. *Journal of Geophysical Research: Atmospheres*, 125(13). Available from: <https://doi.org/10.1029/2020jd032835>
- Steinfeld, D. & Pfahl, S. (2019) The role of latent heating in atmospheric blocking dynamics: a global climatology. *Climate Dynamics*, 53(9), 6159–6180. Available from: <https://doi.org/10.1007/s00382-019-04919-6>
- Swanson, K.L. (2002) Dynamical aspects of extratropical tropospheric low-frequency variability. *Journal of Climate*, 15(16), 2145–2162. Available from: [https://doi.org/10.1175/1520-0442\(2002\)015<2145:DATOETL>2.0.CO;2](https://doi.org/10.1175/1520-0442(2002)015<2145:DATOETL>2.0.CO;2)
- Wang, Z., Li, M., Shaoqing Zhang, R., Small, J., Lv, L., Yuan, M. et al. (2023) The Northern Hemisphere wintertime storm track simulated in the high-resolution community earth system model. *Journal of Advances in Modeling Earth Systems*, 15(10), e2023MS003652. Available from: <https://doi.org/10.1029/2023MS003652>
- Weijenborg, C., de Vries, H. & Haarsma, R.J. (2012) On the direction of Rossby wave breaking in blocking. *Climate Dynamics*, 39(12), 2823–2831. Available from: <https://doi.org/10.1007/s00382-012-1332-1>
- Woollings, T., Hannachi, A. & Hoskins, B.J. (2010) Variability of the North Atlantic eddy-driven jet stream. *Quarterly Journal of the Royal Meteorological Society*, 136, 856–868. Available from: <https://doi.org/10.1002/qj.625>
- Zhang, K., Wan, H., Liu, X., Ghan, S.J., Kooperman, G.J., Ma, P.-L. et al. (2014) Technical note: on the use of nudging for aerosol-climate model intercomparison studies. *Atmospheric Chemistry and Physics*, 14(16), 8631–8645. Available from: <https://doi.org/10.5194/acp-14-8631-2014>

SUPPORTING INFORMATION

Additional supporting information can be found online in the Supporting Information section at the end of this article.

How to cite this article: Boljka, L., Bethke, I., Tao, D., & Li, C. (2024). Upstream influence of midlatitude jet stream biases in boreal summer. *Atmospheric Science Letters*, 25(12), e1272. <https://doi.org/10.1002/asl.1272>